Supplementary Information

Flame Growth of Nickel-based Cocatalyst for Efficient Solar Water Splitting of $BiVO_4$ Photoanode

Haohua Wang [a], Youyi Su [a], Xiangui Pang [a], Ming Zhang [b], Wufang Wang [a], Pingping Yang [a], Xinxin Lu [c*], and Jiale Xie [a, d*]

[a] School of New Energy and Materials, Southwest Petroleum University, Chengdu, 610500, People's Republic of China.

[b] School of Chemistry and Chemical Engineering, Southwest Petroleum University, Chengdu 610500, People's Republic of China.

[c] Hydrogen Energy R&D Department, PetroChina Shenzhen New Energy Research Institute Co., Ltd., Shenzhen 518054, P.R. China.

[d] Key Laboratory of Advanced Energy Materials Chemistry (Ministry of Education), Nankai University, Tianjin 300071, P.R. China.

*Corresponding author. X. X. Lu, E-mail: lu.xinxin6391@gmail.com; J. L. Xie, E-mail: jialexie@swpu.edu.cn

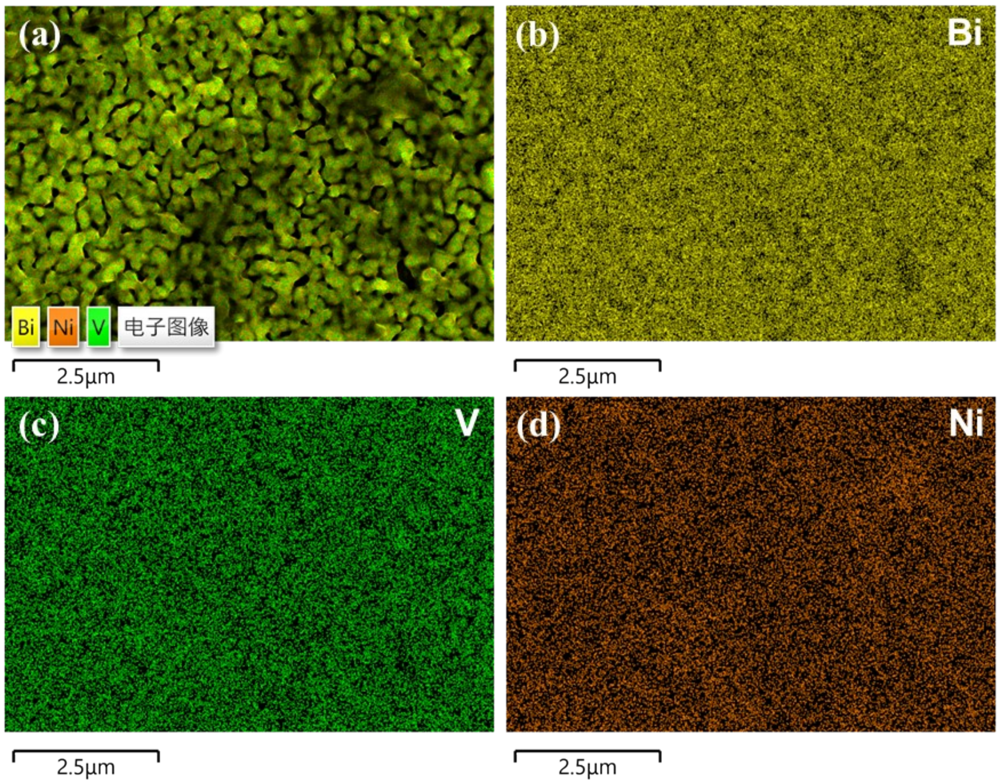

Figure S1. (a) SEM image and EDS mappings overlapped image of the as-prepared NiO_x/BVO photoanode. (b) EDS mapping of Bi element. (c) EDS mapping of V element. (d) EDS mapping of Ni element.

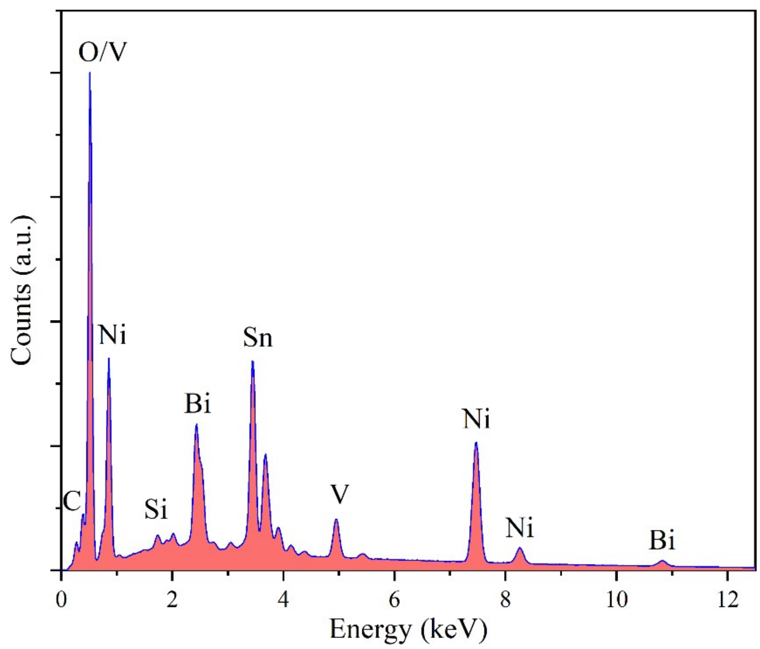

Figure S2. EDS pattern of the as-prepared NiO_x/BVO photoanode.

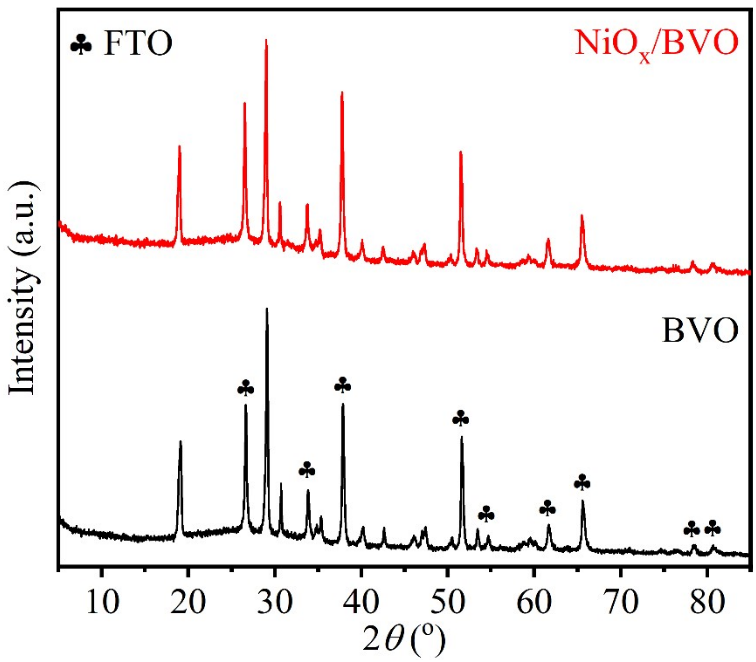

Figure S3. XRD patterns of the as-prepared BVO and NiO_x/BVO photoanodes.

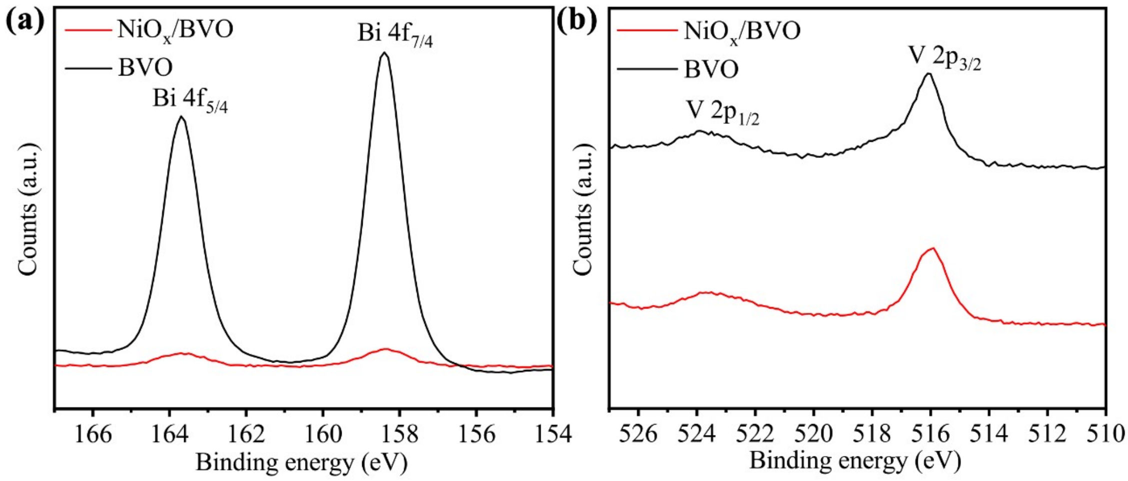

Figure S4. (a) Bi 4f XPS spectra of the BVO and NiO_x/BVO photoanodes. (b) V 2p XPS spectra of the BVO and NiO_x/BVO photoanodes.

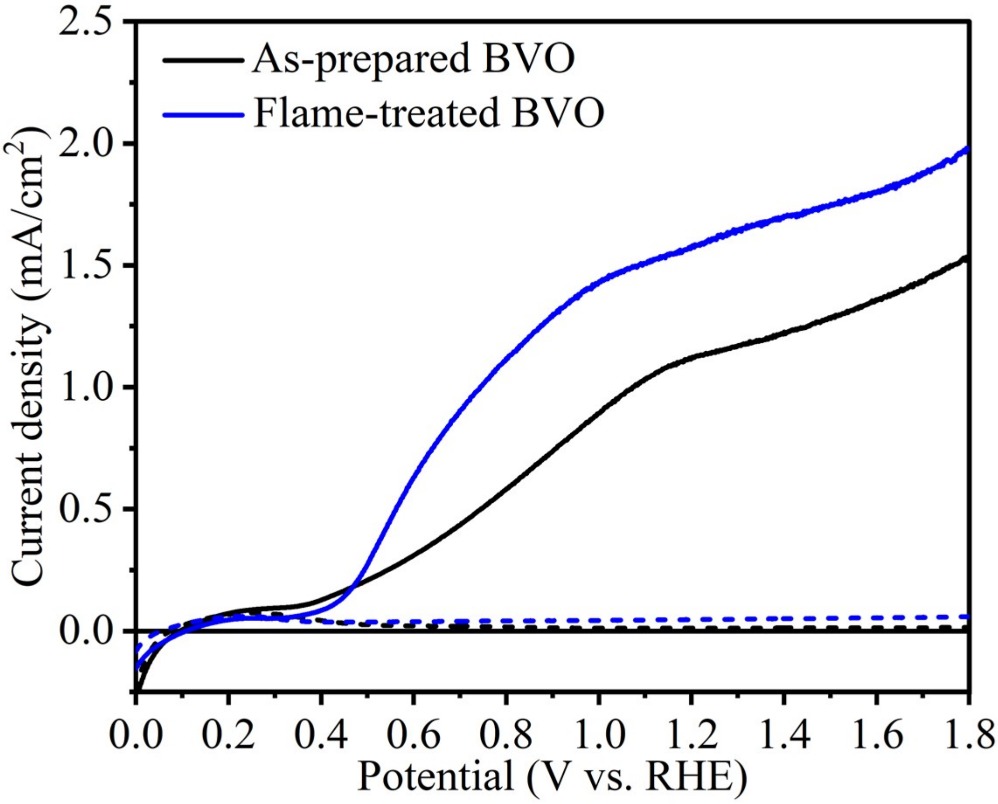

Figure S5. LSV curves of the as-prepared and flame-treated BVO photoanodes at a scan rate of 20 mV/s.

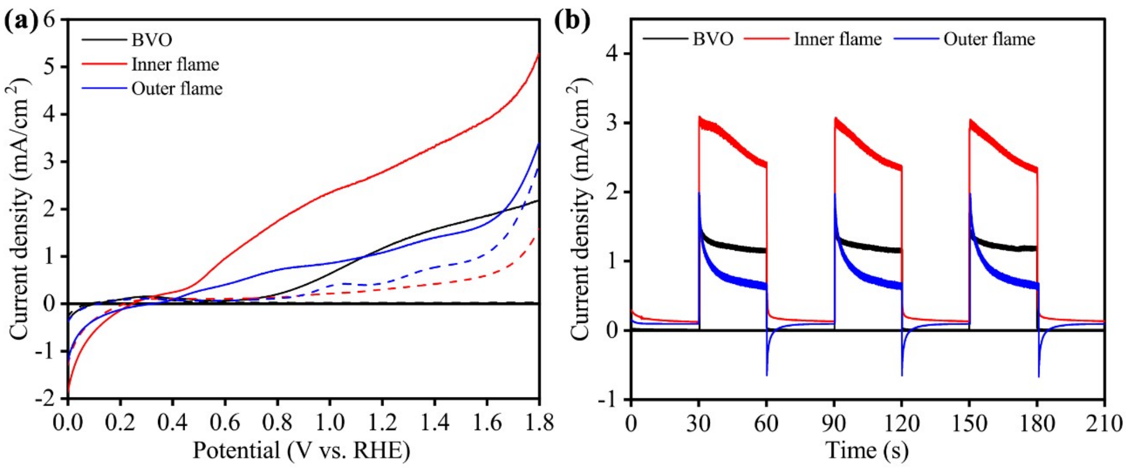

Figure S6. (a) LSV curves and (b) *J*-*t* plots of the BVO and NiO_x/BVO photoanodes with different flame treatments.

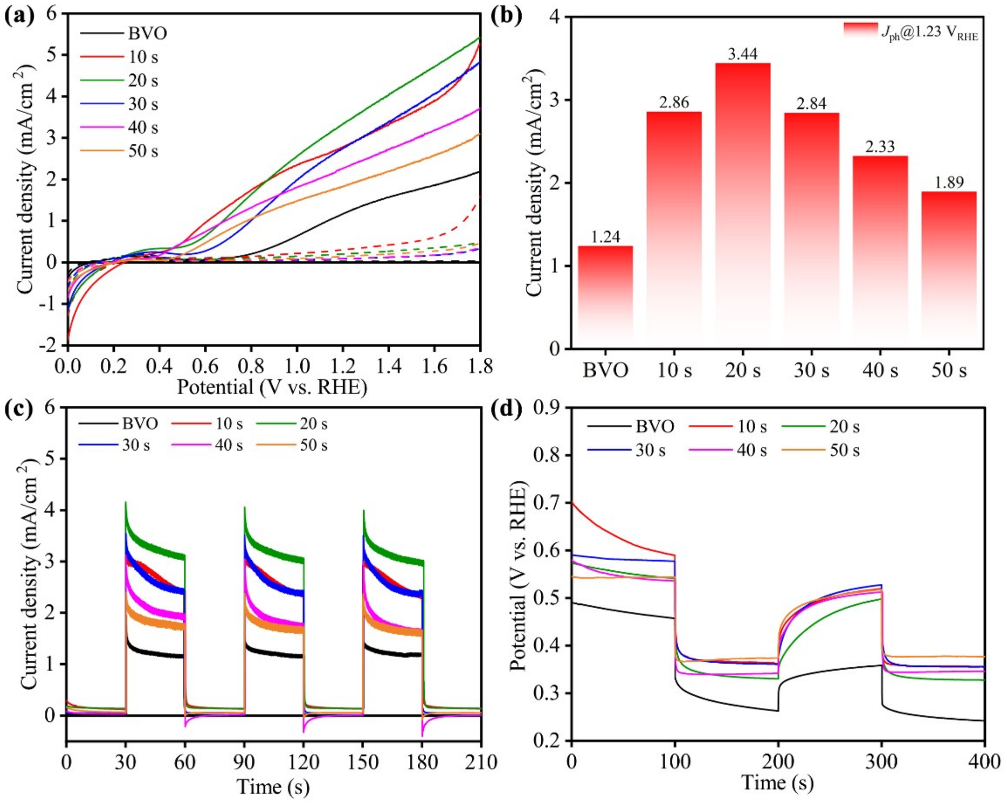

Figure S7. (a) LSV, (c) *J-t*, and (d) OCPT plots of the BVO and NiO_x/BVO photoanodes with various flame treatment times. (b) Photocurrent density of the BVO and NiO_x/BVO photoanodes at 1.23 V vs. RHE.

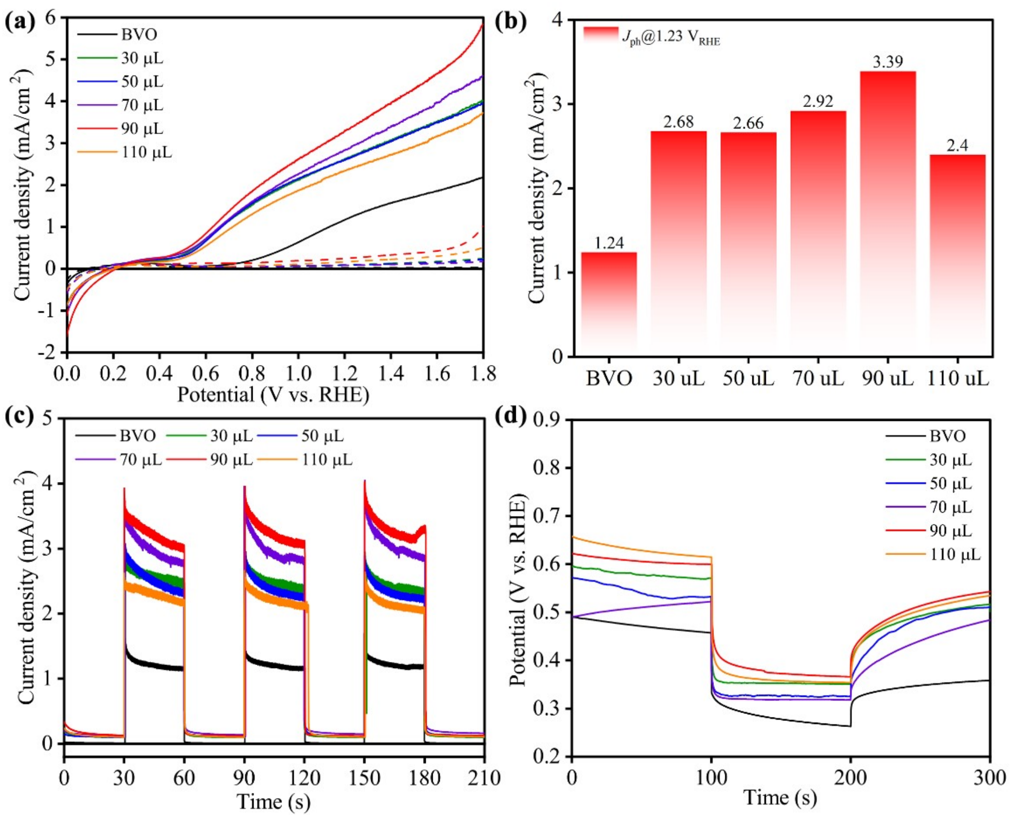

Figure S8. (a) LSV, (c) *J-t*, and (d) OCPT plots of the BVO and NiO_x/BVO photoanodes with various volumes of $Ni(NO_3)_2$ ethanol solution. (b) Photocurrent density of the BVO and NiO_x/BVO photoanodes at 1.23 V vs. RHE.

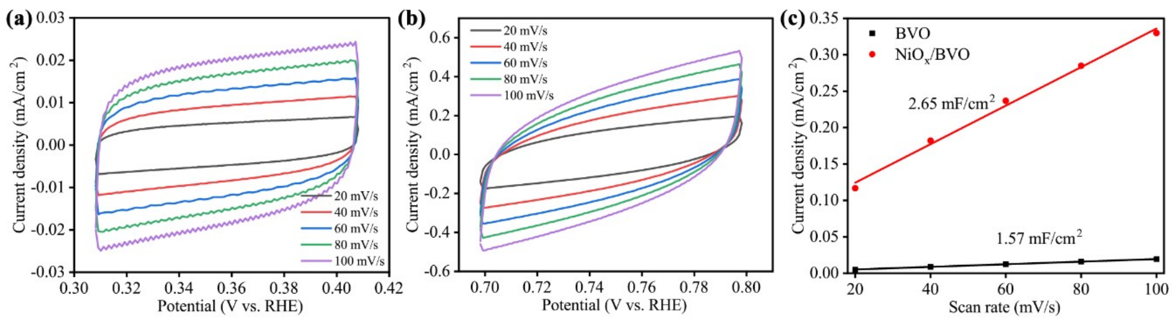

Figure S9. (a) CV curves of the BVO photoanode. (b) CV curves of the NiO_x/BVO photoanode. (c) ECSA of the BVO and NiO_x/BVO photoanodes.

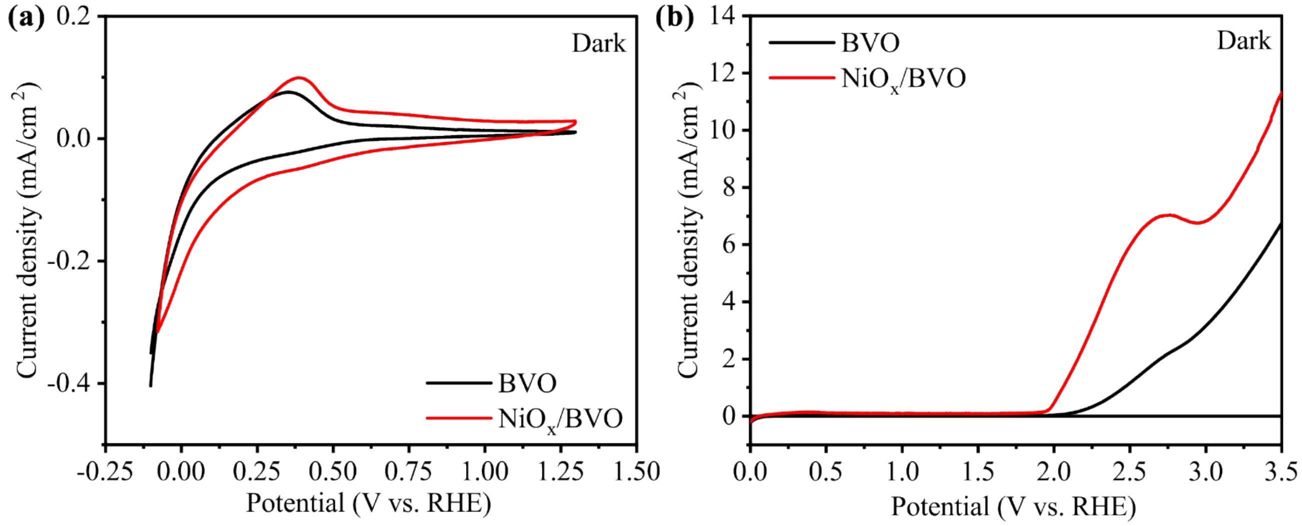

Figure S10. (a) CV curves of the BVO and NiOx/BVO photoanodes in the dark at a scan rate of 100 mV/s. (b) LSV curves of the BVO and NiOx/BVO photoanodes in the dark at a scan rate of 20 mV/s.

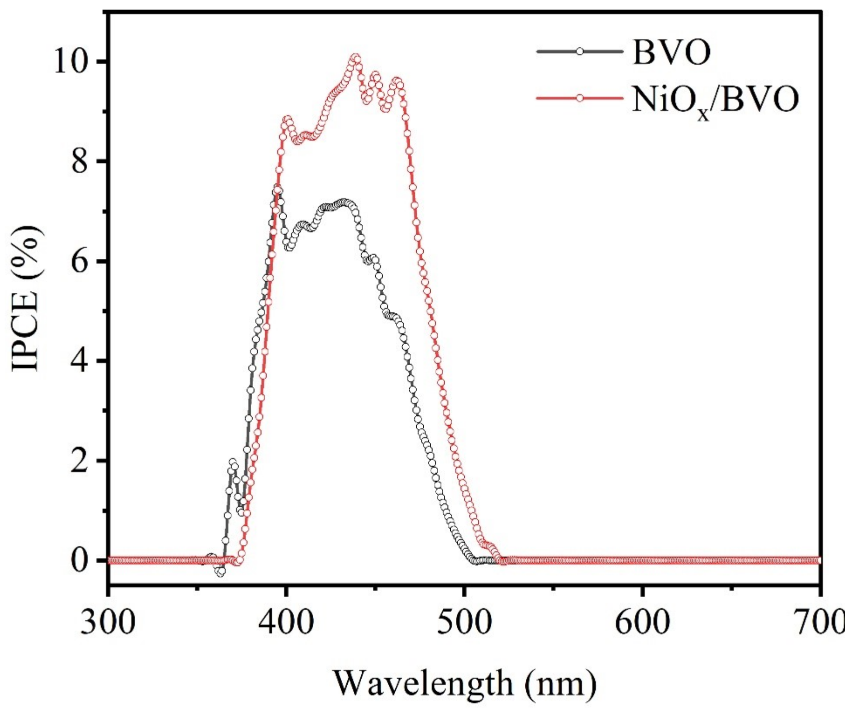

Figure S11. IPCE of NiO_x/BVO and BVO photoanodes measured with two-electrode configuration without bias. The electrolyte is the phosphate buffer (PBS) solution (pH = 6.86).

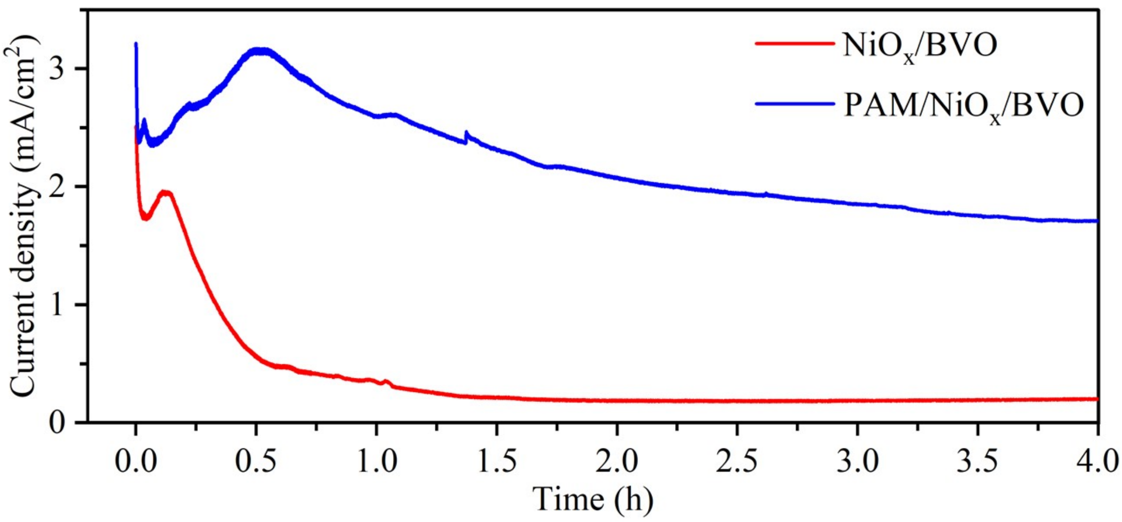

Figure S12. PEC stability of the NiO$_x$/BVO and PAM/NiO$_x$/BVO photoanodes during the initial 4 h.

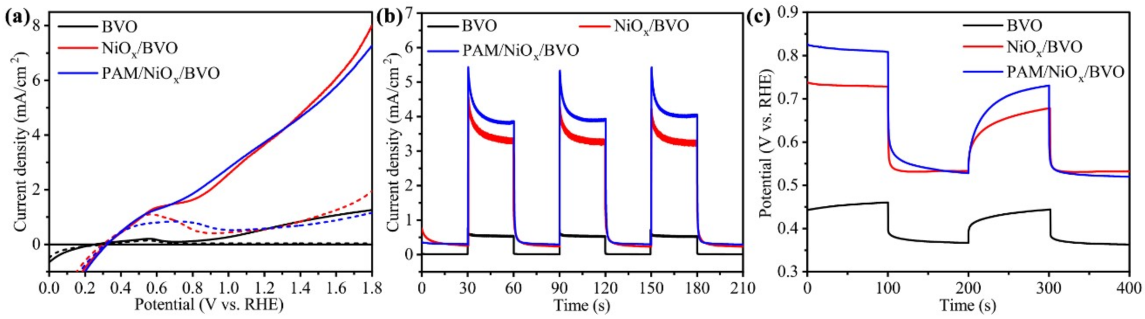

Figure S13. PEC performance of the PAM/NiO$_x$/BVO photoanode. (a) LSV curves at a scan rate of 20 mV/s. (b) *J-t* plots. (c) OCPT plots under the chopped light.

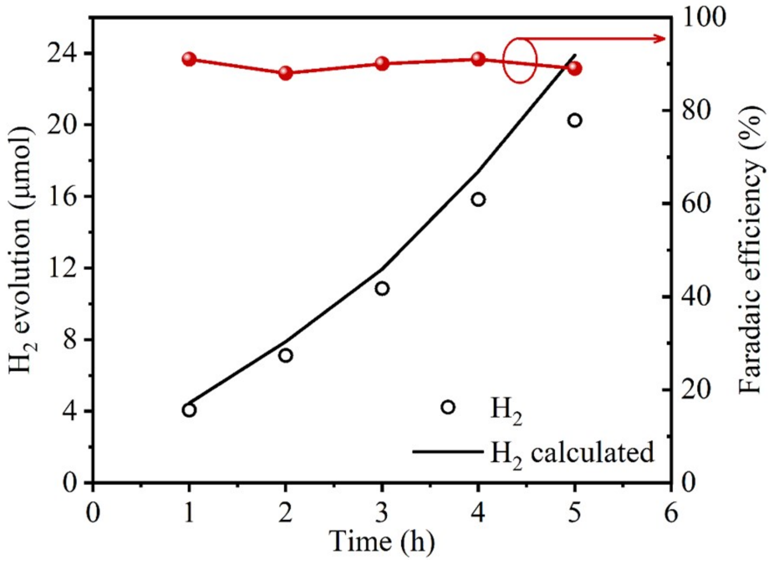

Figure S14. Hydrogen evolution plot and Faradaic efficiency of PAM/NiO$_x$/BVO photoanode at 1.23 V vs. RHE under AM 1.5G illumination.

Table S1. Typical NiO_x and CoO_x cocatalysts synthesized with the different methods for BVO photoanode modification and their performances.

Photoanode	**Synthesis method of cocatalyst**	**Testing conditions**	**Photocurrent at 1.23 V vs. RHE**	**Enhancement factor**	**Ref.**
NiO_x/BVO	Spin-coating and flame synthesis	AM 1.5G (100 mW/cm^2), 0.1 M PBS (pH = 6.86), 20 mV/s	3.80 mA/cm^2	6.67	This work
NiO_x/BVO	Spin-coating and annealing	AM 1.5G (100 mW/cm^2), 1 M KBi (pH = 9.5), 50 mV/s	3.32 mA/cm^2	2.86	1
NiO_x/Mo:BVO	Photochemical-metal-organic deposition method	AM 1.5G (100 mW/cm^2), 0.5 M Na_2SO_4 (pH = 6.8), 20 mV/s	2.44 mA/cm^2	2.07	2
CoO_x/BVO	Immersion and annealing	AM 1.5G (100 mW/cm^2), 0.1 M KPi (pH = 7), 10 mV/s	~1.5 mA/cm^2	~1.36	3
NiO_x/BVO	Electrodeposition	AM 1.5G (100 mW/cm^2), 0.5 M KBi (pH = 9.2), 10 mV/s	3.19 mA/cm^2	2.14	4
NiOOH/BVO	Immersion	AM 1.5G (100 mW/cm^2), 1 M Na_2SO_4 (pH = 5.92), 10 mV/s	2.70 mA/cm^2	~2.30	5

References

1. X. Cao, L. X. Ren, Y. B. Zhao, H. H. Chen, Z. Q. Lu, Y. Liu, S. J. Wei, Q. Ma, L. B. Zhong, L. J. Song and Y. J. Qiu, *Chemical Engineering Journal*, 2025, **510,** 161859.
2. M. Zhang, R. P. Antony, S. Y. Chiam, F. F. Abdi and L. H. Wong, *ChemSusChem*, 2019, **12**, 2022-2028.
3. M. Zhong, T. Hisatomi, Y. Kuang, J. Zhao, M. Liu, A. Iwase, Q. Jia, H. Nishiyama, T. Minegishi, M. Nakabayashi, N. Shibata, R. Niishiro, C. Katayama, H. Shibano, M. Katayama, A. Kudo, T. Yamada and K. Domen, *Journal of the American Chemical Society*, 2015, **137**, 5053-5060.

4. S. Wang, Z. Shi, K. Du, Z. Ren, H. Feng, J. Wang, L. Wang, D. Cui, Y. Du and W. Hao, *Small Methods*, **n/a**, 2401443.
5. H. Luo, C. Liu, Y. Xu, C. Zhang, W. Wang and Z. Chen, *International Journal of Hydrogen Energy*, 2019, **44**, 30160-30170.